withdraws the ruthenium center's intrinsic valence-shell electron, and the reduction potentials are largely due to the π-acceptor ability of the ligands in ruthenium(II) complexes.[19,20] Thus, the electrochemical properties show that π-acceptor ability increases in the order Cl < Br < NCS < CN.

The tendency observed in the SIMS spectra of proton affinity to increase in the examined complexes was consistent with that of the $t_2 \rightarrow \pi^*$ transition energy and $E_{1/2}$.

From measurement of the electronic spectrum for $[Ru(CN)_2(bpy)_2]$ in strongly acidic solution, Schilt reported that the nitrogen atom of the cyanide group was the most likely site for protonation.[6] We thought that a proton would bind to the anionic ligands because the electronegativity of the ligands increases to the extent that the π-acceptor property of the ligands increases in the complexes.

For low-volatility and thermally unstable complexes such as $[RuX_2(bpy)_2]$ in which the ruthenium atom has seven stable isotopes with comparatively large abundances, a difference in proton affinity between the complexes arising from replacement of monodentate anionic ligands was found from measurement of liquid SIMS spectra. Pattern analysis is a useful and powerful method for correlating the results obtained from liquid SIMS spectra with characteristics of the complexes obtained by other methods.

Acknowledgment. We wish to express our sincere thanks to Dr. Shinzaburo Hishida (Hitachi, Ltd.) for his helpful suggestions.

(19) Connor, J. A.; Meyer, T. J.; Sullivan, B. P. *Inorg. Chem.* **1979**, *18*, 1388.
(20) Johnson, C. R.; Shepherd, R. E. *Synth. React. Inorg. Met.-Org. Chem.* **1984**, *14*, 339.

Contribution from the Department of Chemistry, Texas A&M University, College Station, Texas 77843

X-ray Powder Structure and Rietveld Refinement of the Monosodium-Exchanged Monohydrate of α-Zirconium Phosphate, $Zr(NaPO_4)(HPO_4)\cdot H_2O$

Philip R. Rudolf and Abraham Clearfield*

Received August 8, 1988

The crystal structure of the partially hydrated monosodium-exchanged phase of α-zirconium phosphate, $Zr(HPO_4)_2\cdot H_2O$, has been determined by using data collected on a conventional computer-controlled X-ray powder diffractometer. The positions of all atoms in the layer were determined by using 40 unambiguously indexed reflections, obtained by pattern decomposition, in a conventional single-crystal type analysis. Whole-pattern (Rietveld) analysis was then conducted to $R_{wp} = 0.156$ and resulted in the location and refinement of the exchanged Na^+ ion and the water oxygen in the interlamellar space. $Zr(NaPO_4)(HPO_4)\cdot H_2O$ is monoclinic, $P2_1/c$, with cell parameters $a = 8.8264$ (2) Å, $b = 5.3494$ (1) Å, $c = 16.0275$ (6) Å, $\beta = 101.857$ (4)°, and $Z = 4$. The structure is a modification of the parent α-zirconium phosphate with a shift of adjacent layers and twisting of the phosphate groups. This results in an altered cavity arrangement. Na^+ lies in a distorted octahedral environment, as does the water oxygen, O12. This arrangement of atoms in the interlamellar region is in an ordered manner similar to that in $Zr(NH_4PO_4)_2\cdot H_2O$. Loss of the 1 mol of water results in a change in space group, and a mechanism for this transformation as well as that of the exchange process will be described.

Introduction

Zirconium bis(monohydrogen orthophosphate) monohydrate, $Zr(HPO_4)_2\cdot H_2O$ or α-ZrP, is a microcrystalline powder with a layered structure.[1] The phosphate hydrogens may be exchanged for mono- and divalent cations, resulting in a large number of half-exchanged and fully exchanged phases.[2] For each exchange ion there exists a number of phases that represent different hydrates as well as anhydrous phases.[2,3]

In the parent α-ZrP[1,4] the Zr atoms lie nearly in a plane and are bridged by the phosphate groups, which alternate above and below the level of the plane. Three oxygens of each phosphate group are bonded to three different zirconium atoms arranged at the apices of a near-equilateral triangle. The fourth oxygen points away from the layer and into the interlamellar region. These oxygens, labeled O7 and O10, are bonded to protons. Adjacent layers are staggered, resulting in hexagonal-capped cavities between the layers. A water molecule resides in the center of each cavity. The adjacent layers are held together solely by van der Waals forces, and they are able to expand or contract as a result of ion exchange or intercalation processes. The ion-exchanged zirconium phosphates are readily identified by their characteristic basal *d*-spacing in the X-ray powder pattern, and relationships between basal *d*-spacing and the amount of water of crystallization in the structure are well-known.[5]

Single crystals of α-ZrP may be prepared by a variety of methods.[1,6] However, ion exchange on such crystals results in loss of some crystallinity as the layers disorder.[7] Retention of the crystalline structure on ion exchange is accomplished by exchanging microcrystalline α-ZrP in buffered solutions by slow potentiometric titration.[8,9] The product is a microcrystalline powder. However, even when good-quality single crystals are used for exchange, the product is so disordered that it cannot be used for structure solutions by standard single-crystal methods. Thus, the single-crystal structure of only one exchanged phase, $Zr(NH_4PO_4)_2\cdot H_2O$, has been obtained previously.[10] This structure solution was possible because ammonia is taken up by intercalation rather than ion exchange and forms ammonium ions at the proton sites.[11] Apparently, the intercalation process with a small molecule does not greatly disorder the layers as the resultant phase was found to have a structure very similar to that of the parent acid.

Given the problem with the exchanged phases, we undertook to solve their structures by powder methods.[12,13] To make the

* To whom correspondence should be addressed.

(1) Clearfield, A.; Smith, G. D. *Inorg. Chem.* **1969**, *8*, 431.
(2) Clearfield, A. Zirconium Phosphates. In *Inorganic Ion Exchange Materials*; Clearfield, A., Ed.; CRC Press: Boca Raton, FL, 1982; p 16.
(3) Clearfield, A.; Duax, W. L.; Medina, A. S.; Smith, G. D.; Thomas, J. R. *J. Phys. Chem.* **1969**, *73*, 3424.
(4) Troup, J. M.; Clearfield, A. *Inorg. Chem.* **1977**, *16*, 3311.
(5) Alberti, G. *Acc. Chem. Res.* **1978**, *11*, 163.
(6) Alberti, G.; Torracca, E. *J. Inorg. Nucl. Chem.* **1968**, *30*, 317.
(7) Alberti, G.; Costantino, U.; Giulietti, R. *J. Inorg. Nucl. Chem.* **1980**, *42*, 1062.
(8) Clearfield, A.; Medina, A. S. *J. Inorg. Nucl. Chem.* **1970**, *32*, 2775.
(9) Clearfield, A.; Duax, W. L.; Garces, J. M.; Medina, A. S. *J. Inorg. Nucl. Chem.* **1972**, *34*, 329.
(10) Clearfield, A.; Troup, J. M. *J. Phys. Chem.* **1973**, *77*, 243.
(11) Alberti, G.; Bertrami, R.; Costantino, U.; Gupta, J. P. *J. Inorg. Nucl. Chem.* **1977**, *39*, 1057.
(12) Rudolf, P. R. Ph.D. Dissertation, Texas A&M University, May 1983.

0020-1669/89/1328-1706$01.50/0

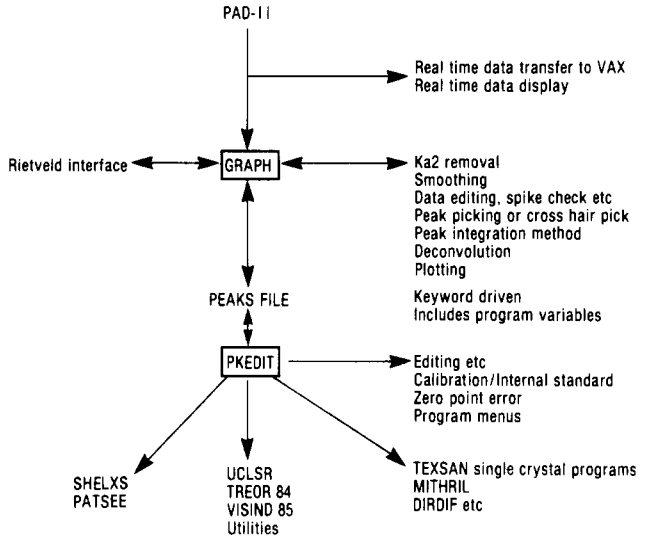

Figure 1. Schematic representation of the programs used for indexing, cell refinement, and preparation of data for structural analysis by Rietveld and single-crystal program sets.

methods of general applicability, programs were prepared that allow for ab initio structure solutions.[13] This technique was applied to the solution of the structures of $Zr(KPO_4)(HPO_4)$[14] and $Zr(NaPO_4)(HPO_4)$.[13] These phases crystallize in a space group different from that of the parent α-ZrP. The change in space group arises from a translation of the layer at $^1/_2c$ by $^1/_2b$. A neutron diffraction study of $Zr(KPO_4)(HPO_4)$[15] unambiguously located the hydrogen atom and confirmed that the structure determined from X-ray powder data was correct.

In a continuation of this previous work, we report a new program set[16] used in solving structures from X-ray powder data and show how this is applied to the monosodium monohydrate ion-exchanged phase $Zr(NaPO_4)(HPO_4)\cdot H_2O$. This compound slowly loses water in humidities of less than 30% or under long X-ray exposure. Previous work on the use of X-ray powder data for structure solutions, by other authors, has been extensively cited in ref 12–15.

Experimental Section

Sample Preparation. Zirconium phosphate gel[17] was prepared by slowly adding, with vigorous stirring, concentrated H_3PO_4 to a 0.5 M $ZrOCl_2\cdot 8H_2O$ solution. The gel was allowed to stand for 12 h and then filtered and washed free of Cl^- with distilled, deionized water. After air-drying, microcrystalline 12:336 α-ZrP was prepared by refluxing the dry gel in 12 M H_3PO_4 for 336 h. The sodium half-exchanged phase was prepared by potentiometric titration using 0.1 M NaOH/NaCl at a pH less than 6.0 to ensure that there was no phosphate group hydrolysis or formation of the fully exchanged phase. Equilibration was ensured by stirring the exchanged powder in the mother liquor over a period of 7 days. $Zr(NaPO_4)(HPO_4)\cdot 5H_2O$ was isolated by filtering and converted to $Zr(NaPO_4)(HPO_4)\cdot H_2O$ on air-drying with equilibration above 30% relative humidity. The starting material was identified by its basal d spacing.

X-ray Data Collection and Structure Solution. $Zr(NaPO_4)(HPO_4)\cdot H_2O$ was finely ground in an agate mortar and ca. 5% of NBS standard Si powder (SRM No. 640) was added as an internal calibrant. This homogeneous mixture was then placed into a closed environment sample holder[12] with enough water added to maintain the relative humidity above 30% during data collection. The purpose of the calibrant was to offset any zero-point error introduced by the sample holder. One day was allowed for equilibration, and step scan data were then collected between 5 and 80° 2θ with a step size of 0.01° 2θ and count time of 32 s.

A Seifert-Scintag automated powder diffractometer (PAD-II) with Cu Kα Ni-filtered radiation (λ = 1.541 84 Å) was used for data collection. Data were transferred in real time to a MicroVAX-II-based system where data processing and analysis was conducted. A schematic of the programs[14] used in the data collection and analysis is given in Figure 1.

The "GRAPH" series of programs is a menu-driven program set that allows the operator to carry out each of the required operations and to examine the results at every step of the way. It includes data editing, smoothing, plotting, and pattern decomposition programs.[14] The latter program was developed with the help of Dr. L. F. Guseman, Jr., and R. Sparks of the Texas A&M University mathematics department. Essentially, it consists of a new approach that involves maximum likelihood estimation (MLE) techniques, with mixtures of normal densities.[18] GRAPH also interfaces to prewritten program sets such as TEXSAN, SHELXS, and the X-ray 82 Rietveld program so that data may be transferred back and forth at every stage of the structure solution and refinement. A more complete description will be presented later.

Data were mathematically stripped of the Kα_2 contribution[19] after being checked for spikes, and peak picking was conducted by a modification of the double-derivative method.[20] The peaks list were processed by program PKEDIT and a linear calibration correction of ca. 0.04° 2θ applied to the peak positions. Two low-angle peaks were eliminated, as they resulted from ca. 0.5% contamination from the dehydrated phase, $Zr(NaPO_4)(HPO_4)$.

Indexing was carried out by trial and error[21] and Ito methods,[22] resulting in a monoclinic cell close to that finally refined. Indices were automatically assigned from low to high angle during unit cell least-squares refinement.

Systematic absences of the type $h0l$, $l = 2n + 1$, and $0k0$, $k = 2n + 1$, fixed the space group unambiguously as $P2_1/c$. A total of 40 unambiguous reflections were determined (as single indexed peaks) at this stage, and their accurate intensities were measured by decomposition (MLE) methods, after which they were used as a minimal data set in the TEXSAN[23] series of single-crystal programs. Direct methods (MITHRIL)[24] and automatic Patterson map interpretation were both used to locate the zirconium atom and one of the phosphorus atoms. The atoms were then used as a known fragment in DIRDIF,[25] and additional atoms were located by using the weighted Fourier synthesis section of this program. During this procedure the remaining phosphorus and the eight phosphate oxygen atoms were located and refined. These 11 atoms were used as the starting structure for Rietveld refinement.[26]

In Rietveld refinement a total of 41 geometric constraints were identified for the atoms within the layer, and these were used for an initial distance/angle least-squares refinement. Rietveld refinement proceeded first with refinements on the scale, zero-point, and cell parameters. This was followed by refinement of the four peak shape parameters. The zero-point error refined immediately to ca. 0.04° 2θ. Areas containing the Si calibrant reflections and the two observable peaks of the anhydrous phase were not included in the refinement. After the initial cycles the positional and thermal parameters were refined in a weighted manner between the profile intensities and the geometric constraints. The lower the weighting factor, the more the refinement is based upon the intensities relative to the geometric constraints. The weighting factor in the early stages of refinement was high (25.0) and was lowered as the refinement progressed. The final weighting factor was 3.0.

During the course of the refinement, difference Fourier methods were used to successfully locate both Na^+ and the water oxygen. They were included in the refinement and refined first positionally and, in the last stages of refinement, thermally, together with thermal parameter refinement of the atoms forming the layers. No geometric constraints were

(13) Rudolf, P. R.; Clearfield, A. *Acta Crystallogr.* **1985**, *B41*, 418.
(14) Clearfield, A.; McCusker, L. B.; Rudolf, P. R. *Inorg. Chem.* **1984**, *23*, 4679.
(15) Rudolf, P. R.; Clearfield, A. *Inorg. Chem.* **1985**, *24*, 3714.
(16) Rudolf, P. R. "The GRAPH System of Powder Programs", Texas A&M University, College Station, TX, 1988. Inquiries should be addressed to P.R.R., Inorganic Group, Analytical Sciences, 1897 Building, The Dow Chemical Co., Midland, MI 48667, or A.C., Department of Chemistry, Texas A&M University, College Station, TX 77843.
(17) Clearfield, A.; Oskarsson, Å.; Oskarsson, C. *Ion Exch. Membr.* **1972**, *1*, 91.
(18) Guseman, L. F., Jr.; Bryant, J. In *Pulse Cytophotometry III*; Lutz, D., Ed.; European Press: Ghent, Belgium, 1978; pp 78–92.
(19) Ladell, J.; Zagofsky, A.; Pearlman, S. *J. Appl. Crystallogr.* **1975**, *8*, 499.
(20) Mallory, C. L.; Snyder, R. L. *Adv. X-ray Anal.* **1979**, *23*, 121.
(21) Werner, P.-E. *Z. Kristallogr.* **1965**, *120*, 375.
(22) Visser, J. W. *J. Appl. Crystallogr.* **1969**, *2*, 89.
(23) "TEXSAN: TEXRAY Structure Analysis Package for Single Crystal Data"; Molecular Structure Corp.: The Woodlands, TX, 1986; revised 1987.
(24) Gilmore, G. J. "MITHRIL: A Computer Program for the Automatic Solution of Crystal Structures from X-ray Data", University of Glasgow, Scotland, 1983.
(25) Beurskens, P. T. "DIRDIF: Direct Methods for Difference Structures", Technical Report 1984/1, Crystallography Laboratory, Toernooiveld, 6525 ED Nijmegen, The Netherlands.
(26) Baerlocher, Ch. "The X-ray Rietveld System", version of Sept 1982, Institut fuer Krist. and Petrographie, ETH, Zurich, Switzerland. Modified for VAX/VMS, Texas A&M University, 1984.

Table I. Crystallographic Data

pattern range (2θ), deg; steps	10–80; 6233
step scan increment (2θ), deg	0.01
step scan count time, s	36
standard peak for starting profile: 2θ deg; *hkl*; *R*	11.23; 002; 0.018
space group	$P2_1/c$; $Z = 4$
a, Å	8.8264 (2)
b, Å	5.3494 (1)
c, Å	16.0275 (6)
β, deg	101.857 (4)
no. of contributing reflcns	412
no. of geometric observns	41
8 P–O dists, Å	1.53 (2)
6 Zr–O dists, Å	2.06 (2)
12 O–P–O angles, deg	109.5 (2.0)
12 O–Zr–O angles, deg	90.0 (2.0)
3 O–Zr–O angles, deg	180.0 (3.0)
zero-point error (2θ), deg	0.0409
no. of structural params	45
no. of profile params	9
statistically expected R_{wp}	0.155
$R_{wp} = [\sum w_i(Y_o - Y_c/c)^2/\sum w_i Y_o^2]^{1/2}$	0.156
$R_F = (\sum\|I_o^{1/2} - I_c^{1/2}\|)/(\sum I_o^{1/2})$	0.131
$R_p = \sum[Y_i(\text{obs}) - Y_i(\text{calc})]/\sum[Y_i(\text{obs}) - \text{bkgd}_i]$	0.196

Table II. Final Positional and Thermal Parameters and Their Esd's for $Zr(NaPO_4)(HPO_4)\cdot H_2O$

atom	*x*	*y*	*z*	B_{iso},[a] Å^2
Zr	0.7419 (11)	0.7584 (46)	0.9716 (6)	1.24 (8)
P1	0.106 (2)	0.756 (8)	0.112 (1)	1.90 (11)
P2	0.656 (2)	0.264 (6)	0.093 (1)	
O1	−0.035 (3)	0.771 (14)	0.035 (2)	1.46 (15)
O2	0.206 (7)	0.526 (9)	0.101 (3)	
O3	0.205 (7)	1.001 (9)	0.117 (3)	
O4	0.698 (7)	0.528 (8)	0.064 (3)	
O5	0.521 (3)	0.746 (14)	0.908 (2)	
O6	0.695 (6)	0.0552 (7)	0.038 (3)	
O7	0.040 (4)	0.725 (15)	0.194 (2)	
O10	0.250 (5)	0.706 (12)	0.318 (2)	
O12	0.783 (6)	0.754 (28)	0.224 (4)	3.43 (20)
Na	0.497 (4)	0.213 (15)	0.280 (3)	7.32 (19)

[a] Temperature factors for like atoms located within the layer were constrained to be the same.

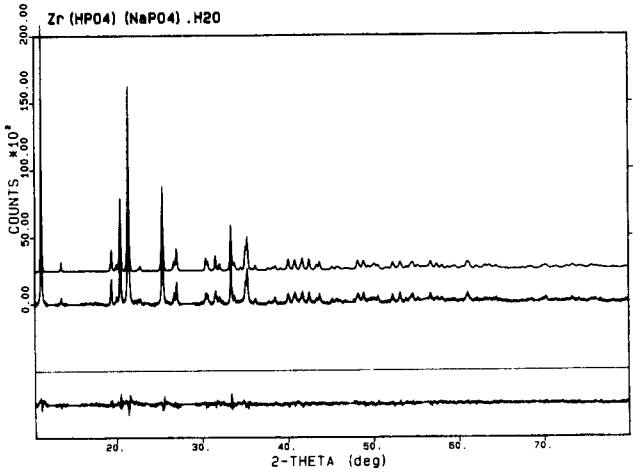

Figure 2. Final Rietveld refinement plot (X-ray intensity versus 2θ) for $Zr(NaPO_4)(HPO_4)\cdot H_2O$: calculated trace (top); observed plot (middle); difference plot (bottom). The difference trace is on the same scale as that of the observed and calculated data.

made on the sodium or water oxygen. Thermal parameters for like atoms within the layer were constrained to be the same to reduce the number of variables relative to the available data.

At this stage of the refinement R_{wp} was ca. 21%. Final adjustments to the background contribution, and to the profile parameters in small regions, followed by further refinement, yielded rapid convergence with $R_{wp} = 0.156$, $R_e = 0.155$, $R_F = 0.131$, and $R_p = 0.196$. To check the correctness of the water O12 and Na positions, their positional parameters were interchanged after the final convergence. Rerefinement showed that the *R* factors remained about the same; however, the temperature factor for water O12 dropped to 0.2 and that for Na became 12.5. This is a strong indication that the initial assignments for Na and water O12 were correct.

Table III. Interatomic Distances (Å) and Angles (deg) and Their Esd's for $Zr(NaPO_4)(HPO_4)\cdot H_2O$

	av value	min/max
Zr–O	2.021 (6)	2.00 (5)/2.04 (5)
P–O	1.547 (7)	1.50 (5)/1.57 (6)
O–Zr–O	180 (2)	177 (2)/184 (2)
O–Zr–O	90 (2)	88 (2)/94 (2)
O–P–O	109.5 (15)	104 (3)/114 (3)

	dist	direction		dist	direction
Na–Na	2.84 (11)	*b*	O7–O10	2.43 (5)	*ac*
Na–O10	2.98 (6)	*ac*	O7′–O12	2.42 (7)	*a*
Na–O12	2.46 (6)	*a*	O10–O12	2.51 (16)	*b*

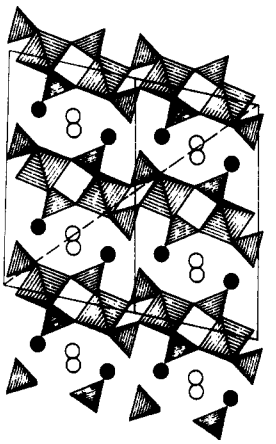

Figure 3. Polyhedral representation of $Zr(NaPO_4)(HPO)_4\cdot H_2O$ unit cell projected along *b*, showing water oxygens (black circles) and sodium ions (open circles) residing between the layers. The dashed line shows the *c* axis based upon the original proton form, α-ZrP, with its *a* axis equal to $-a$.

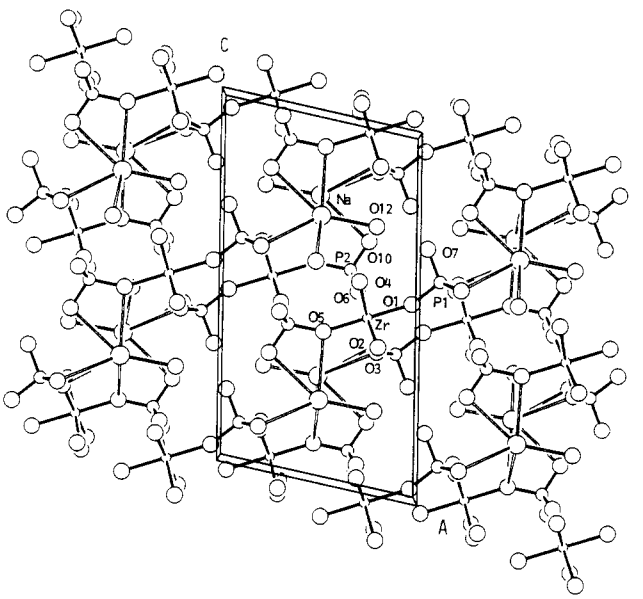

Figure 4. Schematic drawing of the $Zr(NaPO_4)(HPO_4)\cdot H_2O$ structure, showing the numbering scheme to identify the atoms. O12 represents the water molecule, and O7 and O10 are the phosphate oxygens bonded to protons in α-ZrP.

Results

Table I lists the crystallographic data, Table II the positional and thermal parameters, and Table III the important bond distances and angles for $Zr(NaPO_4)(HPO_4)\cdot H_2O$. The final Rietveld refinement plot is given in Figure 2. Figure 3 shows a polyhedral

representation of the structure, while Figure 4 shows the actual atom arrangement and numbering scheme.

The unit cell chosen to describe the structure is not the same one used for the parent α-ZrP structure. The relationship between the two cells is as follows: If the present unit cell is represented by a, b, c and the α-ZrP cell by A, B, C, then $A = -a$, $B = -b$, and $C = c + 2a$, which results in unit cell parameters of A = 8.8264 Å, B = 5.3494 Å, C = 21.2658 Å, and β = 132.47°. Application of the transformation matrix then gives the new positional parameters in terms of the old as $X = -x + 2z$, $Y = -y$, and $Z = z$. The new c axis is outlined in Figure 3 by dashed lines.

$Zr(NaPO_4)(HPO_4)\cdot H_2O$ retains essentially the same layer structure as the parent α-ZrP. However, the phosphate groups are twisted so that the P–OH groups do not point toward the Zr atoms in adjacent layers. This twist has the effect of producing alternating wide and narrow passages within each layer and a slight contraction of the a axis (a = 9.060 (2) Å in α-ZrP[4]). The sodium ions (open circles in Figure 3) reside in the wide cavities at approximately $^1/_4$ and $^3/_4b$ and slightly above and below $^1/_4c$ and $^3/_4c$ with an interatomic separation of 2.84 Å (Table II). Each sodium ion is loosely held, being surrounded by six atoms and ions in a distorted octahedral arrangement. There are two Na^+ at distances of 2.84 (11) Å, O10 at 2.98 (6) Å, O5 at 2.99 (6) Å, O2 at 3.08 Å, and the water oxygen, O12, at a distance of 2.46 (6) Å. O5 and O2 are phosphate oxygens that bridge to Zr atoms whereas O10 is bonded to a proton in the parent α-ZrP. Thus, as will become evident in what follows, the Na^+ were exchanged for the O10 protons.

It should also be noted that O10 and O5 are part of the same phosphate group and thus have a chelating arrangement relative to Na^+. This comes about by the phosphate group rotating in such a way that the P–O10 direction points away from Na^+ and toward O7. This twist brings the O5 atom closer to the Na^+ ion. At the same time, the O7 phosphate group also is rotated so that the P–O7 direction is no longer perpendicular to the layer, but directed toward O10. Two other framework oxygens, O5′ and O3 are at distances of 3.18 and 3.20 Å, respectively, completing the shielding of the sodium ions.

Each water molecule, represented by black circles in Figure 3, is also octahedrally coordinated, albeit in a highly distorted fashion, with the coordination consisting of atoms O10 (2.51 (16) Å), O10′ (3.01 (16) Å), O7 (2.42 (10) Å), O3 (2.86 (10) Å), O4 (2.80 (9) Å), and Na (2.46 (6) Å). The O7 oxygen is the other proton-bearing phosphate oxygen in α-ZrP. The positions of the Na^+ and water molecule roughly correspond to the positions of N1 and N2, respectively, in $Zr(NH_4PO_4)_2\cdot H_2O$.[10] The ammonium ion structure is more regular in that the phosphate groups are directed almost perpendicular to the layer direction rather than skewed as in Figures 3 and 4. This skewing or twisting of the phosphate groups must result from repulsions set up between Na^+ and the protons on O7. Added evidence for the arrangement P1–O7–H is obtained from an earlier neutron diffraction study of $ZrKH(PO_4)_2$.[15] In that study the proton was clearly shown to be bonded to O7.

There are two short oxygen–water interatomic distances indicative of the hydrogen-bonding scheme. Considering the water molecule at approximately $^3/_4$, $^3/_4$, $^1/_4$ (x, y, z values), there is close contact with O10′ located at $^3/_4$, 1.206, 0.182. Since O10 has no proton, the water oxygen must be the donor. A second short contact (2.41 Å) is made with O7′ located at 1.04, 0.725, 0.194, and in this case O7 is the donor. This hydrogen bond is directed roughly parallel to a, whereas the first one is in the b direction. It would then be expected that a water lone pair is directed toward the Na^+ ion at 0.503, 0.713, 0.220. This would require that the remaining water hydrogen would not be involved in hydrogen bonding but rather is pointed toward framework oxygens. This hydrogen-bonding scheme is somewhat similar to that for the water molecule in α-ZrP.[4,27]

(27) Albertson, J.; Oskarsson, Å.; Tellgren, R.; Thomas, J. O. *J. Phys. Chem.* **1977**, *81*, 1574.

Discussion

It may seem strange that the Na^+ ions align themselves in rows along the b direction at distances of 2.84 Å apart. Under these conditions the ion–ion repulsion should be large. However, it is offset partly by the $[P2–O10]^-\cdots Na^+$ attraction and the close approach of the water molecule. This positioning of the sodium ions places them as far as possible from the P1–O7–H protons and shields the protons through hydrogen bonding to the water from the exchanged ions. In fact, there seems to be a fine balance of forces, with the exchanged sodium ions being very loosely held. Except for the water molecule, the other oxygen atoms are close to 3 Å away from the Na^+ ions, indicative of weak binding. This is also reflected in the large temperature factor observed for the sodium ions. This fine balance of forces is further reflected in the ready loss of the water molecule in a low-humidity atmosphere.[3] In the anhydrous phase[13] the sodium ions are aligned along the a axis at distances of $^1/_2a$ apart. The sodium ions in this structure are now equally coordinated by O10 and O7 atoms and are far apart from each other. Thus, the driving force for dehydration must lie in the alleviation of the Na^+–Na^+ repulsion forces in the monohydrate.

$Zr(KPO_4)(HPO_4)\cdot H_2O$ dehydrates even more readily than the sodium ion phase. Furthermore, its X-ray powder pattern is very similar to that of the corresponding sodium ion phase.[9] Assuming that the structures of the two half-exchanged phases are isomorphous, one would expect that the mutual repulsion of the K^+ ions is even stronger than those experienced by the sodium ions. Hence, the greater is the tendency to dehydrate so that rearrangement to a more stable structure may occur. This close positioning of the exchanging ions also explains why Rb^+ and Cs^+ do not exchange in acid solution with crystalline α-ZrP.[28–31] In the first instance these ions are too large to negotiate the passageways or openings into the α-ZrP structure.[3] However, even when base is added to remove protons and allow the layers to swell, the Rb^+ and Cs^+ ion phases have structures different from those described here. In the case of Cs^+ the first end point occurs at the composition $ZrCs_{1.5}H_{0.5}(PO_4)_2\cdot H_2O$. Given the large ionic radii of Rb^+ and Cs^+ ions, it would be impossible for them to form a phase in which these ions are 2.84 Å apart. A stable phase of composition $ZrCs_{0.5}H_{1.5}(PO_4)_2\cdot H_2O$ has also been reported.[31] In this phase the cesium ions would be separated by at least the b-axis distance, minimizing repulsion between ions.

It is now possible to visualize the sequence of events that occurs on dehydration of the sodium and potassium monohydrates. As a result of ion–ion repulsion, the water molecule leaves the crystal lattice and the exchange ions (Na^+ or K^+) then immediately shift into positions that alleviate the ion–ion repulsions.

It is also instructive to consider the exchange reaction from the point of view of the idealized model developed earlier for α-ZrP.[3] In that model adjacent layers were arranged in such a way as to form hexagonal-shaped cavities as shown in Figure 4 of ref 1. Considering the idealized version of one of the layers as shown in Figure 3 of ref 1, it is easy to visualize how the cavities are formed. The P2–O10 groups run in rows parallel to the b axis and alternate along a, with rows of P1–O7 groups. In the adjacent layer, the P–O groups are rotated 60° so that they are roughly above the Zr atoms in the layer below. The rows of O10 and O7 atoms still alternate along a and run parallel to b. Thus, two sides of the cavity are bounded by Zr–P2–O10–Zr–P2–O10–Zr atoms, two are bounded similarly by O7 atoms, and two are bounded by mixed O10–O7 arrangements. Calculations show[3] that the largest free volumes exist in the two sides of the cavity containing O10 atoms only. Thus, the least resistance to diffusion should occur in a zigzag path through these sides of the cavity and parallel to the b axis. This appears to be the diffusion path followed by Na^+ and K^+.

(28) Clearfield, A.; Oskarsson, Å. *Ion Exch. Membr.* **1974**, *1*, 205.
(29) Clearfield, A.; Kullberg, L. H. *J. Phys. Chem.* **1974**, *78*, 1812.
(30) Abertsson, J. *Acta Chem. Scand.* **1966**, *20*, 1689.
(31) Alberti, G.; Costantino, U.; Allulli, S.; Massucci, M. A. *J. Inorg. Nucl. Chem.* **1975**, *37*, 1779.

We may also speculate on the diffusion path followed by the displaced protons. As a Na^+ ion enters the cavity closest to the surface, a proton on O10 is transferred to the water molecule of α-ZrP, which resides in the center of the cavity. This hydronium ion is in turn repelled by the Na^+ ion and moves toward the O7 nearest the surface whereupon the O7 atom gives up its proton to the outer solution. The $[P1-O7]^-$ group then accepts a proton from the hydronium ion. As the sodium ions diffuse further into the layer, a counter diffusion of protons along the O7 path must take place. Since the O7 atoms are one *b* length apart (or 5.35 Å) in the same layer, but about 3.5 Å apart in adjacent layers, the proton can be transferred by rotation of the hydronium ion followed by donation to cover the shorter distance. However, as the sodium ions diffuse inward, water follows to form a pentahydrate with an interlayer spacing of 11.8 Å[3]. Under these conditions the closest O7-O7 distance is *b* and some diffusion as well as rotation of the hydronium ion might occur to effect proton transfer.

In Figure 3 the dashed line indicates the *c* axis in terms of the original α-ZrP cavity. It is seen that the layers appear to be shifted along *a* to create a large β angle. In the fully exchanged ammonium ion form the β angle based on the original cavity is again small (102.7°).[10] The two ammonium ions are situated close to opposite sides of the cavity, one of them being surrounded by three O10 atoms and one O7 atom and the other one by three O7 atoms and one O10 atom. Thus, the layers realign themselves similar to their relative positions in α-ZrP.

It is perhaps fitting at this juncture to emphasize that the structural details emerging from these studies were made possible through the parallel development of ab initio methods of solving crystal structures from X-ray powder data. Our emphasis has been to use these techniques with ordinary diffractometer generated data on equipment that is readily available in every diffraction laboratory as opposed to using synchrotron radiation[32] or film methods.[33] Continuation of efforts in this direction, so as to obtain accurate data to higher 2θ values, should further improve the method and allow structure determinations to be carried out in a fairly routine manner for many situations where single crystals are unobtainable.

Acknowledgment. This work was supported by the Robert A. Welch Foundation, Grant No. A-673, for which grateful acknowledgment is made. We also wish to thank Christian Baerlocher for supplying us with the original Rietveld code.

(32) Attfield, J. P.; Sleight, A. W.; Cheetham, A. K. *Nature* **1986**, *322*, 620.
(33) Berg, J. E.; Werner, P. E. *Z. Kristallogr.* **1977**, *145*, 310.

Contribution from the Department of Chemistry,
State University of New York at Buffalo, Buffalo, New York 14214

Donor-Acceptor Properties of Ambient-Temperature Chloroaluminate Melts

Thomas A. Zawodzinski, Jr.,† and Robert A. Osteryoung*

Received September 29, 1988

The donor-acceptor properties of room-temperature chloroaluminate ionic liquids composed of mixtures of $AlCl_3$ with either *N*-(1-butyl)pyridinium chloride or 1-ethyl-3-methylimidazolium chloride were studied. Gutmann donor and acceptor numbers were determined by using the Eu(III) reduction potential and the ^{31}P chemical shift of triethylphosphine oxide, respectively. Acidic melts are extremely poor donor and strong acceptor media. Basic melts are similar in basicity to DMF. No conclusions concerning the acceptor properties of the basic melt are drawn from this work since the strongly basic probe molecule, $Et_3P{=}O$, is leveled by the solvent. Conditions under which these parameters are potentially useful are outlined.

Introduction

The chemistry observed in ambient-temperature chloroaluminate ionic liquids composed of mixtures of $AlCl_3$ with either *N*-(1-butyl)pyridinium chloride (BuPyCl) or 1-ethyl-3-methylimidazolium chloride (ImCl), generally referred to as RCl, is strongly affected by melt composition.[1] The composition dependence of the chemistry of the ambient-temperature chloroaluminate melts is due to the change of the anionic makeup of the melt with composition. In basic melts, all aluminum chloride added is neutralized by reaction with chloride ion. Thus, only Cl^- and $AlCl_4^-$ ions are present in appreciable quantities in the basic melt. In acidic melts, all of the chloride is neutralized and the excess $AlCl_3$ present forms $Al_2Cl_7^-$. In this composition regime, $AlCl_4^-$ and $Al_2Cl_7^-$ are the principal anionic components of the melt. The character of the melts as solvents is determined by the presence of chloride ion in basic melts and heptachlorodialuminate ions in the acidic melt, as given by the equation

$$2AlCl_4^- \rightleftharpoons Al_2Cl_7^- + Cl^- \quad (1)$$

The most common descriptive construct for acid-base chemistry in molten salts is the anionotropic solvent system model.[2] The properties of solutes are described in terms of the transfer of characteristic anions. A base is a substance that liberates this anion, while an acid consumes it. This concept, a generalization of the Arrhenius acid concept, was first applied in the study of oxide-containing systems by Lux, Flood, and Førland.[3,4] When this concept is applied to chloroaluminates, basic solutes liberate chloride and acidic solutes are chloride acceptors. Melt acidity is defined in terms of the quantity -log $[Cl^-]$, or pCl, of the melt. Unfortunately, this formalism provides no information not known from the equilibrium constant for the anion equilibrium. Furthermore, this description of acidity is entirely medium specific and no information concerning the properties of the melt relative to other solvents is available. Comparisons with other solvent media allow one to have some insight and predictive ability concerning the chemistry of solutes in the melt.

An alternative to the simple specification of melt composition or pCl for describing medium acid-base properties is the specification of suitable solvent parameters. The Gutmann donor[5,6] and acceptor[6,7] number parameters, DN and AN respectively, are simple and widely used solvent basicity and acidity parameters.

† Present address: Department MEE-11, MS D429, Los Alamos National Laboratory, Los Alamos, NM 87545.

(1) Osteryoung, R. A. Organic Chloroaluminate Ambient Temperature Molten Salts. In *Molten Salt Chemistry*; Mamantov, G., Marassi, R., Eds.; Reidel: Dordrecht, The Netherlands, 1987; ASI Series C, Vol. 202, pp 329-364.
(2) Huheey, J. E. *Inorganic Chemistry*, 3rd ed.; Harper and Row: New York, 1983.
(3) Lux, H. *Z. Elektrochem.* **1939**, *45*, 303.
(4) Flood, H.; Førland, T. *Acta Chem. Scand.* **1947**, *1*, 592, 781.
(5) Gutmann, V.; Wychera, E. *Inorg. Nucl. Chem. Lett.* **1966**, *2*, 257.
(6) Gutmann, V. *The Donor-Acceptor Approach to Molecular Interactions*; Plenum Press: New York, 1978.
(7) Meyer, U.; Gutmann, V.; Gerger, W., *Monatsh. Chem.* **1976**, *106*, 1235.

0020-1669/89/1328-1710$01.50/0